Proceedings of the 8th International Conference on MicroManufacturing
University of Victoria, Victoria, BC, Canada, March 25-28, 2013

Hybridizing Micromachining and Microfabrication for Sensor Chips

ICOMM
2013
No.121

N. Moghimian[1], E.A. Etrati[2], M. Sam[3], and R.B.Bhiladvala[4]
[1]Department of Mechanical Engineering & IESVic, University of Victoria, Canada; nima@uvic.ca
[2]Department of Mechanical Engineering & IESVic, University of Victoria, Canada; etrati@uvic.ca
[3]Department of Mechanical Engineering & IESVic, University of Victoria, Canada; samm@uvic.ca
[4]Department of Mechanical Engineering, IESVic & CAMTEC, University of Victoria, Canada; rustomb@uvic.ca

Key Words: MEMS sensors and actuators, microfabrication, packaging, hybrid micromachining, turbulent wall shear stress, thermal and topographical constraints

ABSTRACT

We present an example of packaging a MEMS sensor for measuring fluctuations of the wall shear stress in turbulent fluid flows. For these sensors, topographical and thermal constraints required the development of a hybrid technique for the packaging. This involved standard microfabrication patterning to create the chip, sub-millimetre micro-machining and firing of low thermal conductivity ceramic, combined with shadow-mask-patterned metal film sputtering as well as wire etching, to address the constraints on packaging.

A. HYBRID MICROFABRICATION AND MICROMACHINING

Microelectronic chips with millions of components per cm^2 have been made by a suite of microelectronic fabrication techniques developed over the last few decades. Pattern transfer by lithography, together with subtractive patterning by dry or wet etching, and/or additive patterning by evaporation, sputtering or chemical vapour deposition for thin film growth have been the mainstay of these techniques.

Traditionally, after complete microfabrication of these microchips, their mounting, with required electrical signal exchange paths, as well as mechanical and thermal performance, has been achieved by a separate suite of techniques termed "packaging". Molding of chip-holders, together with ultrasonic wire bonding for connection of leads, are typical techniques used.

While both microfabrication and packaging techniques have acquired maturity and standardization for microelectronic chips, packaging for each type of MEMS sensor or actuator chip presents challenges which must be dealt with individually [1]. Such chips may have to be shielded from harsh environments that contribute noise or promote degradation, and be designed to withstand exposure to environments in which they serve as transducers [2]. Hybrid techniques, which use conventional micromachining (e.g. sub-millimetre milling and drilling) techniques interspersed with steps borrowed from traditional microfabrication techniques, allow greater flexibility, and may be particularly helpful in the coverage of large areas by small-scale sensors, actuators or energy-conversion devices.

B. INTRODUCTION TO GUARD HEATED THERMAL SENSORS FOR TURBULENT WALL SHEAR STRESS

When a fluid such as air or water flows past a solid wall, it exerts a viscous drag force on it, giving rise to the wall shear stress (WSS). If the flow is turbulent, the shear stress signal at a point shows fluctuations over a large range of time scales. Most macroscale flows in nature and technology are turbulent.

The wall shear stress is a fundamental quantity in wall-bounded turbulent flows. The mean value, $\bar{\tau}_w$ and fluid density ρ, yield a velocity scale, $u_* = (\bar{\tau}_w / \rho)$, called the friction velocity. The role of the friction velocity in the collapse of the mean velocity profiles in different regions of wall-bounded turbulent flow gives it a central place in the theory of wall turbulence.

There is a strong need to better understand WSS *fluctuations*, but measuring them has proved to be difficult. Fluctuations in wall shear stress are related to the structure of the fluctuating velocity field in the region very close to the wall. Drag reduction has been shown to be possible by manipulation of the near-wall velocity field, which would allow reduced fossil fuel use for current transportation vehicles. Flow separation and its control can reduce shock loading on wind turbine blades and WSS sensors, which provide a direct measure of local wind force on the blade can be very useful in this context.

Even on large objects spanning tens of metres, such as wind turbine blades, flow control requires well-resolved local fluctuation measurements, and calls for small but robust sensors. Several methods have been investigated for WSS fluctuation measurement –these are classified as direct methods which typically use the displacement of some form of a spring-tethered floating element and indirect methods, which may be optical, electrochemical mass transfer [3] or thermal [3] methods. Each method has some unique advantages and limitations. Indirect methods require a relation between the measured quantity, an electrical signal arising from a heat or mass transfer rate, and the instantaneous WSS. This relation is usually obtained by simplifying the energy or concentration transport equations, which makes it accurate only in a certain range of WSS magnitudes. Direct methods

are free of the errors of indirect calibration. However, they suffer from drawbacks such as dust contamination, pressure sensitivity, sensitivity to acceleration, vibration and thermal expansion. Optical methods, such as the whispering gallery mode resonator are under development, but may not be robust enough for work outside a carefully controlled laboratory environment. Electrochemical sensors provide the best promise for accurate WSS measurement, but require special solution chemistries to be maintained, and are restricted to flows in a laboratory environment. They cannot be used in air flows.

There are several reported studies using thermal WSS sensors. Microfabricated flush-mounted hot-film sensors can be made non-intrusive in the flow. Conventional single -element hot-film sensors consist of a thin-film sensing element on a solid substrate. The temperature of the thin-film is kept constant using a constant temperature anemometry (CTA) system. In CTA, a fast servo-amplifier equipped bridge circuit is used to maintain the electrically heated film, with temperature -sensitive resistance R, at a constant temperature above the fluid ambient temperature. The power needed to maintain the constant temperature is equal to the rate of heat transfer from the film to the fluid flow. Standard CTA circuits are in common use for velocity measurements, and shown to be capable of adequate temporal and spatial resolution.

Single-element hot-film sensors suffer from unwanted, indirect, heat transfer to the flow through the solid substrate. Heat diffusion from the hot-film into the substrate results in heat transfer to the fluid over an area larger than the physical film area. Such sensors therefore suffer from a loss of spatial resolution. The problem is more severe for low conductivity fluids such as air, where the effective sensor length can be over ten times the film length. As shown in a number of earlier reports [6], the heat exchange length also varies significantly with magnitude, becoming larger for low values of WSS. This makes device resolution and sensitivity vary significantly with the magnitude of the WSS fluctuations, a non-linearity in measurement we seek to remove. It also causes phase distortion and spurious amplification of the low frequency end of the spectrum. Overcoming these limitations has been a challenge. Q. Lin et al. [5] studied MEMS thermal sensor including a hot-film placed on a silicon nitride or parylene diaphragm. An air/vacuum pocket beneath the diaphragm separates the sensor from the substrate. They observed the experimental data from their MEMS probes were incongruous with the classical theory used for conventional sensors. Even though the substrate is separated in this case, thermal conductivity of the diaphragm spreads the heat generated in the sensor into a large area, causing loss of spatial resolution. The low thermal capacity of the membrane changes the effective heat exchange area around the sensor rapidly. Strong fluctuations can pick up more heat from the upstream side; whereas, the small fluctuations lead to bigger preheated area.
Earlier analytical and computational studies have shown that in-plane heat conduction in the fluid can also create significant deviations from the calibration relation. This problem becomes worse for small sensors, and thwarts attempts to improve spatial resolution by making sensors as small as microfabrication techniques will allow.

To tackle these errors of single-element hot-film sensors, we have proposed a guard heated sensor design. The difficulties mentioned earlier for single-element sensors can be removed or greatly reduced by using guard-heaters. The idea of guard-heating is that if we force zero temperature gradient around the hot-film probe, we can block unwanted, indirect heat transfer from the probe to the flow through the substrate as well as reduce departures from the assumptions used in deriving the calibration equation, by reducing in-plane conduction in the fluid. This can be done by a guard-heater, which surrounds the hot-film probe, has the same film thickness, and is kept at the same temperature. The guard-heater is connected to a different CTA circuit, enabling us to do the sensing with the hot-film only.

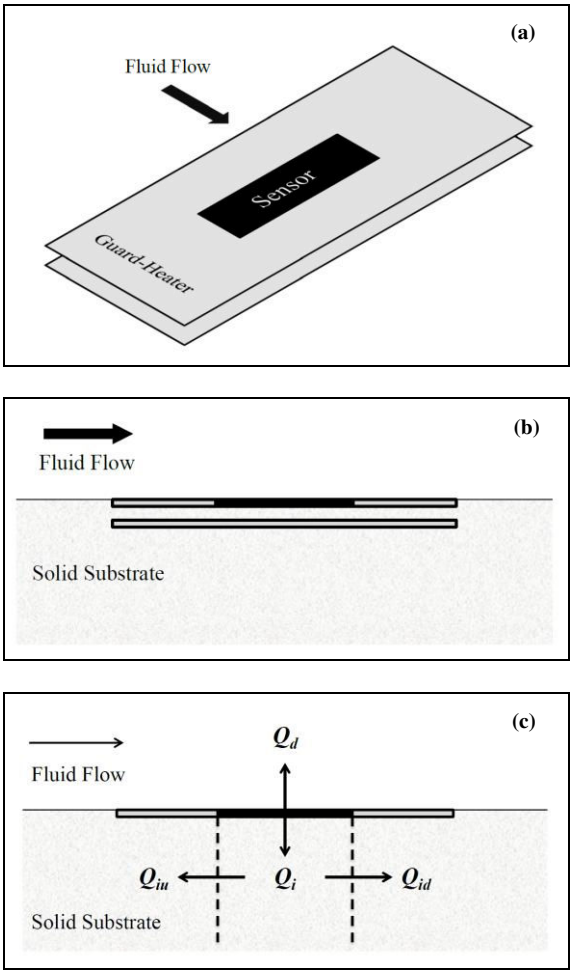

Fig. 1: (a) (b) Two views of a sensor with guard-heating in two planes. (c) A single-plane guard heater made without the lower element, showing direct **(Q_d)** ***and indirect*** **(Q_i)** ***heat transfer paths.***

Figure 1(a) and (b) show the schematic of a guard-heated sensor in two planes. We expect to see zero temperature gradient in the streamwise direction just below the sensor and

guard-heater assembly. However, the temperature gradient in the normal direction, between hot-film and solid substrate still exists. By putting a second guard-heater in the substrate, a few microns below the sensor, we could eliminate normal temperature gradient as well and further reduce the indirect heat transfer. Single-plane guard-heater design, if shown to perform well against the two-plane design, is easier to fabricate and hence, is preferred for the first to attempt for prototype fabrication. A computational analysis helps determine the best location and length of the sensing element within the guard heater –this is chosen so as to maximize the direct heat transport from sensing element to fluid (Q_d) and minimize the indirect heat transfer from the sensing element, through the substrate, to the fluid upstream (Q_{iu}) and downstream (Q_{id}) of the sensor, as shown in Fig. 1(c).

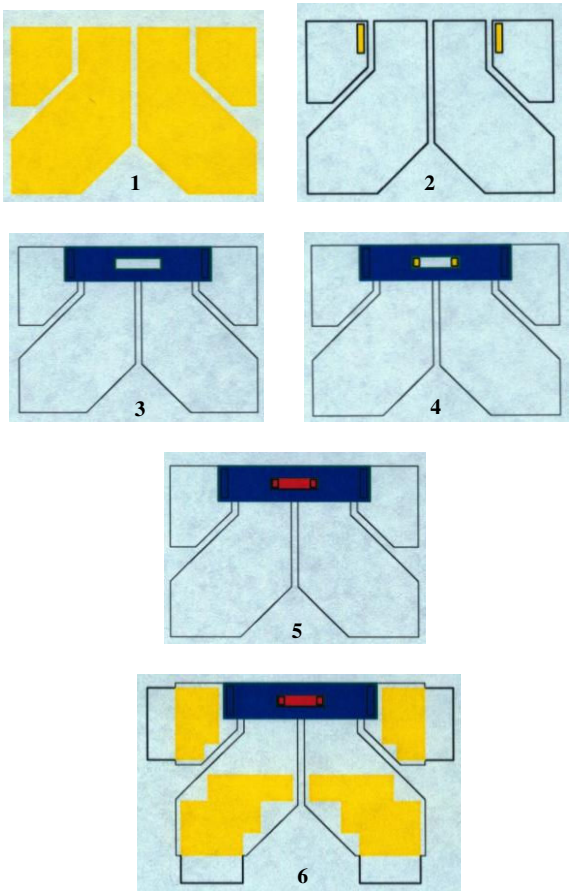

Fig. 2: Six steps of the standard lithographic patterning process used for microfabrication of a guard heated WSS sensor chip. The inner sensing element shown in red is 24 μm x 96 μm. In step (1) four gold bonding pads are created by the first lithographic patterning process followed by gold evaporation and liftoff. At the end of step (6), the exposed gold areas shown on the bonding pads have been connected to the nickel guard heater (outer dark blue rectangle connected to the 2 top pads) and the nickel sensor element (inner red rectangle connected to the 2 bottom pads). The two elements are electrically isolated but thermally contiguous. Details of the steps are in text.

We will now briefly describe the six microfabrication steps required to create the guard heated sensor chip, as shown in Fig. 2. After the first step of creating the four gold bonding pads, a 0.1 μm layer of dielectric silicon oxide is deposited and the lithography step 2 is used to pattern and etch vias through the oxide to allow electrical contact to the gold layer beneath the top two (outer) bonding pads. A lithographic patterning step 3, followed by evaporation of a 0.1 μm nickel film and liftoff, creates the guard heater element, a thin film nickel resistive heater, shown in blue, which will be maintained at constant temperature by one of the CTA circuits. A second layer of dielectric silicon oxide is then deposited and using lithographic patterning step 4, via holes are etched down to the two lower bonding pads. Lithographic step 5 followed by nickel evaporation creates the inner rectangle, the sensing element, shown in red. A capping layer of silicon nitride is then deposited to isolate both elements for use in water, or for making the surface more rugged and resistant to wear. The final lithographic patterning step 6 is used for dry etching to remove the top three layers of dielectric and expose the bonding pads as shown in step (6), to allow connection of the leads. This finishes the wafer-level fabrication. For clarity of steps, the dielectric layers in Fig. 2 have been shown as if they were not transparent. The actual sensor chip is neatly cut from the wafer using a dicing saw, and is shown in the optical micrograph in Fig. 3. The green and purple hue of the sensor and guard heater elements are caused by the different thicknesses of dielectric over them.

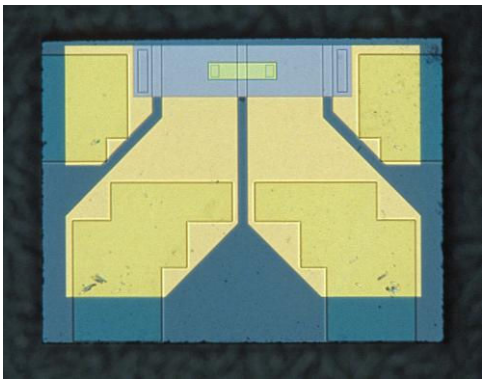

Fig. 3: Fabricated wall shear stress sensor chip(silicon), 1.5 mm x 1 mm. Two nested rectangles at top centre are electrically isolated heating elements, each addressed by two bonding pads.

C. FABRICATION CONSTRAINTS AND HYBRID SCHEME FOR PACKAGING A GUARD HEATED WSS SENSOR

Fig. 3 and caption describe the sensor chip. In this section, we describe the use of sub-millimetre micromaching techniques, milling and drilling. The chip is to be flush mounted within the surface over which fluid flow takes place and show how the packaging process uses a standard microfabrication (sputtering) step for completion. To limit unwanted heat transfer to the substrate, the extent of the high thermal conductivity silicon substrate must be kept small. This is done by securing the chip in a low-thermal conductivity ceramic substrate, shown in Fig. 4. The ceramic, Cotronics 902, was

machined using carbide micromills and microdrills. Drill bits were found to dull and break without completion of a single hole. A dry air jet directed at the drill tip and pecking with small depths of cut were required for the drilling to prevent the drill bits from breaking. The central hole in the ceramic provides a low thermal conductivity air gap over a large fraction of the chip base area. The four chamfered holes around the periphery are to be filled by nailhead-shaped copper wire leads, which exit the back of the cylinder and connect to the driving CTA anemometer circuits. Five finger-like milled protrusions shown in Fig. 4, around the chip boundary are used to wick in low viscosity binder, which is cured to secure the chip in the holder. The as-machined ceramic is fired to a temperature of 2000 ^{o}F, when it changes from a machinable material to one having a hard, porcelain like surface, as seen in Fig. 4.

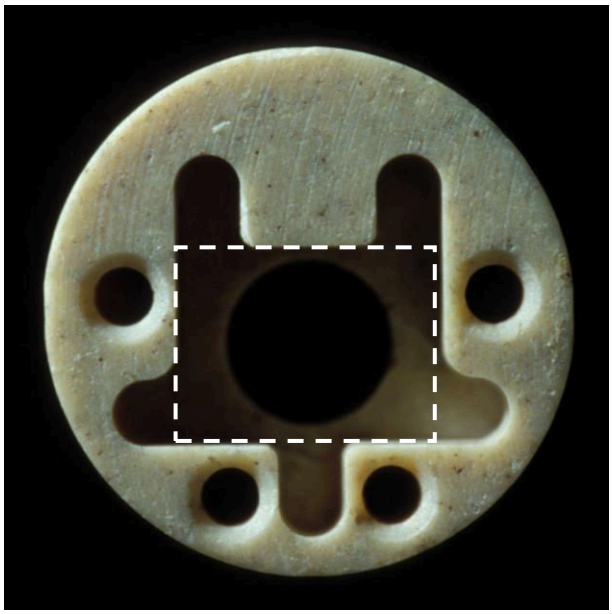

Fig. 4: Cylindrical ceramic (COTRONICS 902) holder, machined using micromilling and microdrilling, then fired and polished. The position of the chip from Fig.3 is shown by the dashed white rectangle.

The topographical requirement is that the chip and holder should present a flat face to ensure no disruption to the fluid flow. This additional constraint on attachment of lead wires to the four on-chip bonding pads, rules out the standard wire-bonding technique, which would involve loops of wire protruding from the chip face.

The alternative used here is to borrow a step of additive patterning from the suite of chip microfabrication processes. A sputtered film of aluminium, about 1 μm thick, is used to create an electrically conductive bridge between each of the four on-chip bonding pads to the four chamfered holes, over the cured binder at the chip-ceramic interface.

How were these bridges patterned? Fig. 5 shows the shadow masks used, micromilled from brass disks using a CNC milling machine. For the shadow masks to work effectively, the patterns must be cut into a thin layer of brass. However, the thin layer would tear or deform during the micromilling process. This led to a design with a thin web supported within a thick brass disk, with a stepped transition of thickness, as seen in Fig. 5.

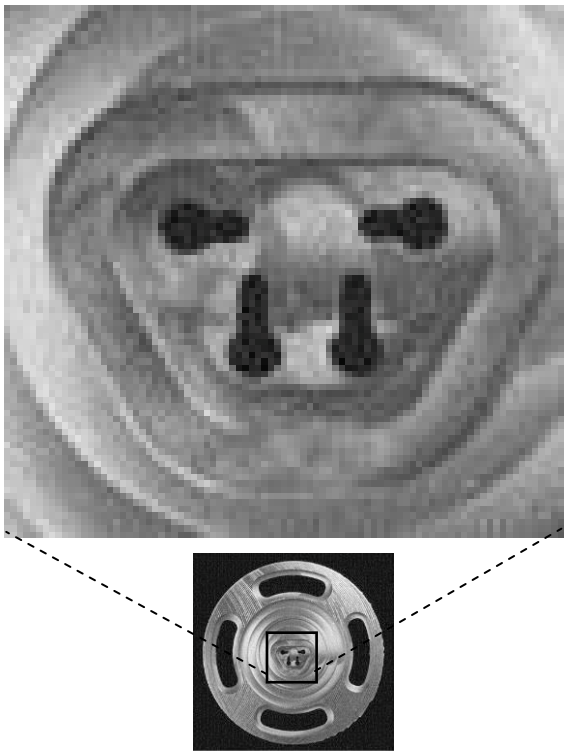

Fig. 5: The shadow mask used to create the four bridges seen in Fig. 6.

The ceramic body with chip secured was mounted in a brass holder and the mask shown in Fig. 5 was aligned with the bonding pads on the secured chip using a stereomicroscope.

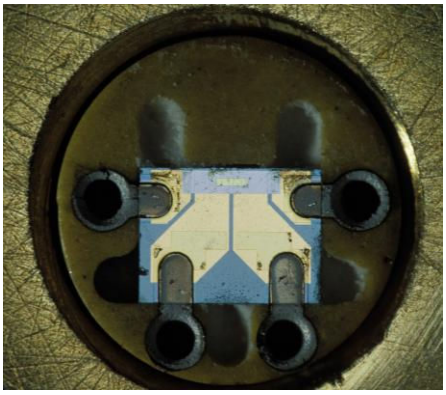

Fig. 6: Sputtered aluminium bridges between each of four on-chip bonding pads and the chamfers of drilled holes in the ceramic.

A sputter tool standard for thin metal film deposition used in

microfabrication, was used to deposit a 1 μm thick film of aluminium, connecting each bonding pad to a chamfered hole. Measurements of aluminium film step height were made by a Tencor Alphastep profile measurement system and recorded. The mounted chip appears as shown in Fig. 6.

Fig. 7: SEM image of transition-etch for copper wire. The wire is cut to the left of the transition line and polished, leaving a 500 μm nailhead transitioning gradually into a 215 μm wire, to drop into the aluminium-coated chamfered holes in Fig. 3.

Nailhead shaped wires made as described by Fig. 7, dropped in from the top face, and secured using conductive silver paste, which provided good electrical contact to the aluminium coated chamfer holes and thus to the chip bonding pads. A mounted sensor has been tested over several hours in a wind tunnel turbulent boundary layer and showed a characteristic turbulent signal, responsive to the flow rate.

D. CONCLUSIONS AND OUTLOOK

In summary, a hybrid packaging scheme borrowing elements of patterned film deposition and etching from the suite of microfabrication techniques, has been developed. This scheme has enabled packaging with special constraints required for this MEMS sensor operation, that are not required in standard microelectronic chips –namely thermal insulation of the chip and the connection of leads in a way that allows presentation of a flat surface for sensor and package, to avoid disruption of the flow being measured. Ongoing work involves experimentation with new fabrication tools to reduce the number of lithography steps and improve step and overall yields.

REFERENCES

[1] C.C. Liu et al., "An assessment of microfabrication to sensor development and the integration of the sensor microsystem," *Microfabricated Systems and MEMS VI,*, Eds: P. Hesketh et al., Electrochem. Soc., Sensors Div., 2002; 1-12.

[2] R. Ramesham et al., "Challenges in interconnection and packaging of microelectromechanical systems (MEMS)," *50th Electronic Components & Technology Conference*, 2000, 666-675.

[3] T. Hanratty et al., in "Fluid Mechanics Measurements", Taylor & Francis, Washington, DC, 1996.

[4] S. Tardu et al., "Response of wall hot-film gages with longitudinal diffusion and heat conduction to the substrate," *Journal of Heat Transfer –Trans. ASME*, 127, 812-819, (2005).

[5] Q. Lin et al., "Experiments and Simulations of MEMS thermal sensors for wall shear stress measurements in aerodynamic control applications," *Journal of Micromechanics and Microengineering*, 14, 1640-1649 (2004).

[6] R.B. Bhiladvala, "Guard heated thermal sensor for wall shear stress fluctuations," 20th International Symposium on Transport Phenomena, 7-10th July, 2009, Victoria, BC, Canada.